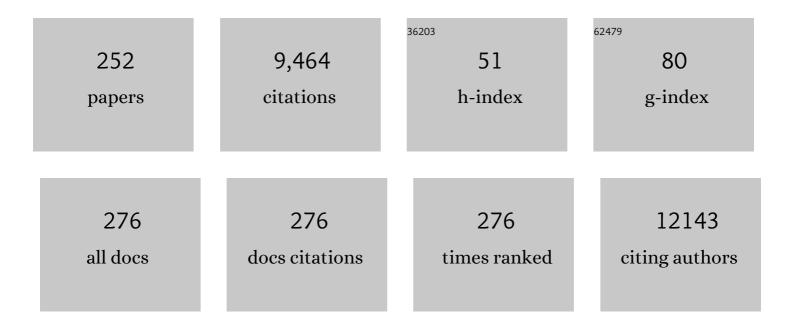
List of Publications by Year in descending order

Source: https://exaly.com/author-pdf/8589690/publications.pdf

Version: 2024-02-01



#	Article	IF	CITATIONS
1	Cellular and molecular neuropathology of the cuprizone mouse model: Clinical relevance for multiple sclerosis. Neuroscience and Biobehavioral Reviews, 2014, 47, 485-505.	2.9	352
2	Proof of concept: enthesitis and new bone formation in spondyloarthritis are driven by mechanical strain and stromal cells. Annals of the Rheumatic Diseases, 2014, 73, 437-445.	0.5	334
3	L1 knockout mice show dilated ventricles, vermis hypoplasia and impaired exploration patterns. Human Molecular Genetics, 1998, 7, 999-1009.	1.4	228
4	More accurate estimation of diffusion tensor parameters using diffusion kurtosis imaging. Magnetic Resonance in Medicine, 2011, 65, 138-145.	1.9	202
5	Functional Connectivity fMRI of the Rodent Brain: Comparison of Functional Connectivity Networks in Rat and Mouse. PLoS ONE, 2011, 6, e18876.	1.1	197
6	Targeted mutation of Cyln2 in the Williams syndrome critical region links CLIP-115 haploinsufficiency to neurodevelopmental abnormalities in mice. Nature Genetics, 2002, 32, 116-127.	9.4	163
7	Common functional networks in the mouse brain revealed by multi-centre resting-state fMRI analysis. NeuroImage, 2020, 205, 116278.	2.1	151
8	Noninvasive in vivo MRI detection of neuritic plaques associated with iron in APP[V717I] transgenic mice, a model for Alzheimer's disease. Magnetic Resonance in Medicine, 2005, 53, 607-613.	1.9	139
9	Elastin fragmentation in atherosclerotic mice leads to intraplaque neovascularization, plaque rupture, myocardial infarction, stroke, and sudden death. European Heart Journal, 2015, 36, 1049-1058.	1.0	139
10	Comparing BOLD fMRI signal changes in the awake and anesthetized rat during electrical forepaw stimulation. Magnetic Resonance Imaging, 2001, 19, 821-826.	1.0	138
11	Different anesthesia regimes modulate the functional connectivity outcome in mice. Magnetic Resonance in Medicine, 2014, 72, 1103-1112.	1.9	136
12	In vivo manganese-enhanced magnetic resonance imaging reveals connections and functional properties of the songbird vocal control system. Neuroscience, 2002, 112, 467-474.	1.1	135
13	Watershed-based segmentation of 3D MR data for volume quantization. Magnetic Resonance Imaging, 1997, 15, 679-688.	1.0	133
14	Evaluation of microwave heating digestion and graphite furnace atomic absorption spectrometry with continuum source background correction for the determination of iron, copper and cadmium in brine shrimp. Journal of Analytical Atomic Spectrometry, 1988, 3, 387.	1.6	125
15	Overexpression of human wildtype torsinA and human ΔGAG torsinA in a transgenic mouse model causes phenotypic abnormalities. Neurobiology of Disease, 2007, 27, 190-206.	2.1	123
16	Diffusion kurtosis imaging probes cortical alterations and white matter pathology following cuprizone induced demyelination and spontaneous remyelination. NeuroImage, 2016, 125, 363-377.	2.1	122
17	Diffusion kurtosis imaging allows the early detection and longitudinal follow-up of amyloid-β-induced pathology. Alzheimer's Research and Therapy, 2018, 10, 1.	3.0	120
18	Magnetic Resonance Imaging and Spectroscopy Reveal Differential Hippocampal Changes in Anhedonic and Resilient Subtypes of the Chronic Mild Stress Rat Model. Biological Psychiatry, 2011, 70, 449-457.	0.7	106

#	Article	IF	CITATIONS
19	Neonatal neuronal overexpression of glycogen synthase kinase-3β reduces brain size in transgenic mice. Neuroscience, 2002, 113, 797-808.	1.1	102
20	The power of using functional fMRI on small rodents to study brain pharmacology and disease. Frontiers in Pharmacology, 2015, 6, 231.	1.6	102
21	Construction and evaluation of multitracer small-animal PET probabilistic atlases for voxel-based functional mapping of the rat brain. Journal of Nuclear Medicine, 2006, 47, 1858-66.	2.8	101
22	Applications of manganese-enhanced magnetic resonance imaging (MEMRI) to image brain plasticity in song birds. NMR in Biomedicine, 2004, 17, 602-612.	1.6	100
23	The Energy Metabolism of Common Carp (Cyprinus carpio) When Exposed to Salt Stress: An Increase in Energy Expenditure or Effects of Starvation?. Physiological and Biochemical Zoology, 2000, 73, 102-111.	0.6	99
24	Current status of functional MRI on small animals: application to physiology, pathophysiology, and cognition. NMR in Biomedicine, 2007, 20, 522-545.	1.6	93
25	Reporter gene-expressing bone marrow-derived stromal cells are immune-tolerated following implantation in the central nervous system of syngeneic immunocompetent mice. BMC Biotechnology, 2009, 9, 1.	1.7	78
26	Mathematical framework for simulating diffusion tensor MR neural fiber bundles. Magnetic Resonance in Medicine, 2005, 53, 944-953.	1.9	77
27	Own-Song Recognition in the Songbird Auditory Pathway: Selectivity and Lateralization. Journal of Neuroscience, 2009, 29, 2252-2258.	1.7	77
28	Early pathologic amyloid induces hypersynchrony of BOLD restingâ€state networks in transgenic mice and provides an early therapeutic window before amyloid plaque deposition. Alzheimer's and Dementia, 2016, 12, 964-976.	0.4	76
29	Current Challenges for the Advancement of Neural Stem Cell Biology and Transplantation Research. Stem Cell Reviews and Reports, 2012, 8, 262-278.	5.6	75
30	1H NMR based metabolomics of CSF and blood serum: A metabolic profile for a transgenic rat model of Huntington disease. Biochimica Et Biophysica Acta - Molecular Basis of Disease, 2011, 1812, 1371-1379.	1.8	73
31	Restoration of MR-induced artifacts in simultaneously recorded MR/EEG data. Magnetic Resonance Imaging, 1999, 17, 1383-1391.	1.0	71
32	Early Changes in Hippocampal Neurogenesis in Transgenic Mouse Models for Alzheimer's Disease. Molecular Neurobiology, 2016, 53, 5796-5806.	1.9	71
33	Hyperpolarized ¹³ C MR metabolic imaging can detect neuroinflammation in vivo in a multiple sclerosis murine model. Proceedings of the National Academy of Sciences of the United States of America, 2017, 114, E6982-E6991.	3.3	71
34	Reduction of ECG and gradient related artifacts in simultaneously recorded human EEG/MRI data. Magnetic Resonance Imaging, 2000, 18, 881-886.	1.0	70
35	Comparisons of different methods to train a young zebra finch (Taeniopygia guttata) to learn a song. Journal of Physiology (Paris), 2013, 107, 210-218.	2.1	69
36	Brain inflammation in a chronic epilepsy model: Evolving pattern of the translocator protein during epileptogenesis. Neurobiology of Disease, 2015, 82, 526-539.	2.1	69

#	Article	IF	CITATIONS
37	Contribution of CYLN2 and GTF2IRD1 to neurological and cognitive symptoms in Williams Syndrome. Neurobiology of Disease, 2007, 26, 112-124.	2.1	67
38	Spatiotemporal properties of the BOLD response in the songbirds' auditory circuit during a variety of listening tasks. Neurolmage, 2005, 25, 1242-1255.	2.1	65
39	Diffusion tensor imaging in a rat model of Parkinson's disease after lesioning of the nigrostriatal tract. NMR in Biomedicine, 2009, 22, 697-706.	1.6	65
40	The autism- and schizophrenia-associated protein CYFIP1 regulates bilateral brain connectivity and behaviour. Nature Communications, 2019, 10, 3454.	5.8	65
41	Proton relaxation enhancement by means of serum albumin and poly-l-lysine labeled with DTPA-Gd3+: Relaxivities as a function of molecular weight and conjugation efficiency. Magnetic Resonance Imaging, 1992, 10, 913-917.	1.0	64
42	Dynamic resting state fMRI analysis in mice reveals a set of Quasi-Periodic Patterns and illustrates their relationship with the global signal. NeuroImage, 2018, 180, 463-484.	2.1	64
43	Evaluation of the specificity and sensitivity of ferritin as an MRI reporter gene in the mouse brain using lentiviral and adeno-associated viral vectors. Gene Therapy, 2011, 18, 594-605.	2.3	63
44	Subtle behavioral changes and increased prefrontal-hippocampal network synchronicity in APPNLâ^'Gâ^'F mice before prominent plaque deposition. Behavioural Brain Research, 2019, 364, 431-441.	1.2	63
45	Neuroanatomy of the fragile X knockout mouse brain studied using in vivo high resolution magnetic resonance imaging. European Journal of Human Genetics, 1999, 7, 526-532.	1.4	61
46	Light Stimulus Frequency Dependence of Activity in the Rat Visual System as Studied With High-Resolution BOLD fMRI. Journal of Neurophysiology, 2006, 95, 3164-3170.	0.9	60
47	A three-dimensional MRI atlas of the zebra finch brain in stereotaxic coordinates. NeuroImage, 2008, 41, 1-6.	2.1	59
48	Quantitative evaluation of MRI-based tracking of ferritin-labeled endogenous neural stem cell progeny in rodent brain. NeuroImage, 2012, 62, 367-380.	2.1	59
49	Microstructural changes observed with DKI in a transgenic Huntington rat model: Evidence for abnormal neurodevelopment. NeuroImage, 2012, 59, 957-967.	2.1	59
50	Diffusion Kurtosis Imaging and High-Resolution MRI Demonstrate Structural Aberrations of Caudate Putamen and Amygdala after Chronic Mild Stress. PLoS ONE, 2014, 9, e95077.	1.1	59
51	<i>In Vivo</i> Morphological Changes in Animal Models of Amyotrophic Lateral Sclerosis and Alzheimer'sâ€Like Disease: MRI Approach. Anatomical Record, 2009, 292, 1882-1892.	0.8	58
52	Resting State fMRI Reveals Diminished Functional Connectivity in a Mouse Model of Amyloidosis. PLoS ONE, 2013, 8, e84241.	1.1	57
53	Targeted intracerebral delivery of the anti-inflammatory cytokine IL13 promotes alternative activation of both microglia and macrophages after stroke. Journal of Neuroinflammation, 2018, 15, 174.	3.1	57
54	Adaptive anisotropic noise filtering for magnitude MR data. Magnetic Resonance Imaging, 1999, 17, 1533-1539.	1.0	56

#	Article	IF	CITATIONS
55	Differential effects of testosterone on neuronal populations and their connections in a sensorimotor brain nucleus controlling song production in songbirds: a manganese enhanced-magnetic resonance imaging study. NeuroImage, 2004, 21, 914-923.	2.1	54
56	Areaâ€ s pecific migration and recruitment of new neurons in the adult songbird brain. Journal of Comparative Neurology, 2010, 518, 1442-1459.	0.9	54
57	Interleukin-13 immune gene therapy prevents CNS inflammation and demyelination via alternative activation of microglia and macrophages. Glia, 2016, 64, 2181-2200.	2.5	53
58	Quinolinic acid injection in mouse medial prefrontal cortex affects reversal learning abilities, cortical connectivity and hippocampal synaptic plasticity. Scientific Reports, 2016, 6, 36489.	1.6	53
59	Brain Responses to Ambient Temperature Fluctuations in Fish: Reduction of Blood Volume and Initiation of a Whole-Body Stress Response. Journal of Neurophysiology, 2005, 93, 2849-2855.	0.9	52
60	Intraneuronal amyloid β and reduced brain volume in a novel APP T714I mouse model for Alzheimer's disease. Neurobiology of Aging, 2008, 29, 241-252.	1.5	52
61	Imaging microglial activation and glucose consumption in a mouse model of Alzheimer's disease. Neurobiology of Aging, 2013, 34, 351-354.	1.5	52
62	MRI visualization of endogenous neural progenitor cell migration along the RMS in the adult mouse brain: Validation of various MPIO labeling strategies. NeuroImage, 2010, 49, 2094-2103.	2.1	51
63	Simultaneous electroencephalographic recording and functional magnetic resonance imaging during pentylenetetrazol-induced seizures in rat. NeuroImage, 2003, 19, 627-636.	2.1	50
64	Structural Changes between Seasons in the Songbird Auditory Forebrain. Journal of Neuroscience, 2009, 29, 13557-13565.	1.7	48
65	Early postnatal behavioral, cellular, and molecular changes in models of Huntington disease are reversible by HDAC inhibition. Proceedings of the National Academy of Sciences of the United States of America, 2018, 115, E8765-E8774.	3.3	47
66	Neural representation of spectral and temporal features of song in the auditory forebrain of zebra finches as revealed by functional MRI. European Journal of Neuroscience, 2007, 26, 2613-2626.	1.2	46
67	Diffusion kurtosis imaging to detect amyloidosis in an APP/PS1 mouse model for Alzheimer's disease. Magnetic Resonance in Medicine, 2013, 69, 1115-1121.	1.9	46
68	Early functional connectivity deficits and progressive microstructural alterations in the TgF344-AD rat model of Alzheimer's Disease: A longitudinal MRI study. Neurobiology of Disease, 2019, 124, 93-107.	2.1	46
69	In vivo dynamic ME-MRI reveals differential functional responses of RA- and area X-projecting neurons in the HVC of canaries exposed to conspecific song. European Journal of Neuroscience, 2003, 18, 3352-3360.	1.2	45
70	Clinical Potential of Intravenous Neural Stem Cell Delivery for Treatment of Neuroinflammatory Disease in Mice?. Cell Transplantation, 2011, 20, 851-870.	1.2	45
71	Seasonal rewiring of the songbird brain: an <i>in vivo</i> MRI study. European Journal of Neuroscience, 2008, 28, 2475-2485.	1.2	41
72	MRI in small brains displaying extensive plasticity. Trends in Neurosciences, 2009, 32, 257-266.	4.2	41

#	Article	IF	CITATIONS
73	A Three-Dimensional Stereotaxic MRI Brain Atlas of the Cichlid Fish Oreochromis mossambicus. PLoS ONE, 2012, 7, e44086.	1.1	41
74	Spatial reversal learning defect coincides with hypersynchronous telencephalic BOLD functional connectivity in APPNL-F/NL-F knock-in mice. Scientific Reports, 2018, 8, 6264.	1.6	41
75	A 3-dimensional digital atlas of the ascending sensory and the descending motor systems in the pigeon brain. Brain Structure and Function, 2013, 218, 269-281.	1.2	40
76	In vivo diffusion tensor imaging (DTI) of brain subdivisions and vocal pathways in songbirds. NeuroImage, 2006, 29, 754-763.	2.1	39
77	In vivo MR imaging of the seasonal volumetric and functional plasticity of song control nuclei in relation to song output in a female songbird. NeuroImage, 2006, 31, 981-992.	2.1	39
78	More from less: high-throughput dual polarity lipid imaging of biological tissues. Analyst, The, 2016, 141, 3832-3841.	1.7	38
79	Impaired Autonomic Regulation of Resistance Arteries in Mice With Low Vascular Endothelial Growth Factor or Upon Vascular Endothelial Growth Factor Trap Delivery. Circulation, 2010, 122, 273-281.	1.6	37
80	Quantitative and phenotypic analysis of mesenchymal stromal cell graft survival and recognition by microglia and astrocytes in mouse brain. Immunobiology, 2013, 218, 696-705.	0.8	37
81	In vivo noninvasive determination of abnormal water diffusion in the rat brain studied in an animal model for multiple sclerosis by diffusion-weighted NMR imaging. Magnetic Resonance Imaging, 1996, 14, 521-532.	1.0	36
82	Cell Type-Associated Differences in Migration, Survival, and Immunogenicity following Grafting in CNS Tissue. Cell Transplantation, 2012, 21, 1867-1881.	1.2	36
83	In-vivo non-invasive study of the thermoregulatory function of the blood vessels in the rat tail using magnetic resonance angiography. NMR in Biomedicine, 2002, 15, 263-269.	1.6	35
84	Neuroplasticity and MRI: A perfect match. NeuroImage, 2016, 131, 13-28.	2.1	35
85	Quasi-Periodic Patterns of Neural Activity improve Classification of Alzheimer's Disease in Mice. Scientific Reports, 2018, 8, 10024.	1.6	35
86	Assessment of the neovascular permeability in glioma xenografts by dynamicT1MRI with Gadomer-17. Magnetic Resonance in Medicine, 2002, 47, 305-313.	1.9	34
87	Identification and characterization of Huntington related pathology: An in vivo DKI imaging study. NeuroImage, 2012, 63, 653-662.	2.1	34
88	Spatiotemporal evolution of early innate immune responses triggered by neural stem cell grafting. Stem Cell Research and Therapy, 2012, 3, 56.	2.4	34
89	Intracerebral transplantation of interleukin 13-producing mesenchymal stem cells limits microgliosis, oligodendrocyte loss and demyelination in the cuprizone mouse model. Journal of Neuroinflammation, 2016, 13, 288.	3.1	34
90	Changing body temperature affects theT2* signal in the rat brain and reveals hypothalamic activity. Magnetic Resonance in Medicine, 2006, 55, 1006-1012.	1.9	33

#	Article	IF	CITATIONS
91	Functional Magnetic Resonance Imaging in Zebra Finch Discerns the Neural Substrate Involved in Segregation of Conspecific Song From Background Noise. Journal of Neurophysiology, 2008, 99, 931-938.	0.9	33
92	Population-averaged diffusion tensor imaging atlas of the Sprague Dawley rat brain. NeuroImage, 2011, 58, 975-983.	2.1	33
93	Functional MRI and functional connectivity of the visual system of awake pigeons. Behavioural Brain Research, 2013, 239, 43-50.	1.2	33
94	Multimodal imaging of subventricular zone neural stem/progenitor cells in the cuprizone mouse model reveals increased neurogenic potential for the olfactory bulb pathway, but no contribution to remyelination of the corpus callosum. NeuroImage, 2014, 86, 99-110.	2.1	33
95	Longitudinal monitoring of metabolic alterations in cuprizone mouse model of multiple sclerosis using 1H-magnetic resonance spectroscopy. Neurolmage, 2015, 114, 128-135.	2.1	33
96	fMRI Reveals a Novel Region for Evaluating Acoustic Information for Mate Choice in a Female Songbird. Current Biology, 2018, 28, 711-721.e6.	1.8	33
97	Non invasive in vivo anatomical studies of the oscine brain by high resolution MRI microscopy. Journal of Neuroscience Methods, 1998, 81, 45-52.	1.3	32
98	Ammonia affects brain nitrogen metabolism but not hydration status in the Gulf toadfish (Opsanus) Tj ETQq0 0	0 rgBT /Ov	erlock 10 Tf
99	In Vivo Monitoring of Adult Neurogenesis in Health and Disease. Frontiers in Neuroscience, 2011, 5, 67.	1.4	32
100	Evaluating the predictive value of doublecortin as a marker for adult neurogenesis in canaries (<i>Serinus canaria</i>). Journal of Comparative Neurology, 2014, 522, 1299-1315.	0.9	32
101	Acute modulation of the cholinergic system in the mouse brain detected by pharmacological resting-state functional MRI. NeuroImage, 2015, 109, 151-159.	2.1	32
102	Neuroimaging of Subacute Brain Inflammation and Microstructural Changes Predicts Long-Term Functional Outcome after Experimental Traumatic Brain Injury. Journal of Neurotrauma, 2019, 36, 768-788.	1.7	32
103	Chemogenetic silencing of neurons in the mouse anterior cingulate area modulates neuronal activity and functional connectivity. NeuroImage, 2020, 220, 117088.	2.1	32
104	Cholinergic and serotonergic modulations differentially affect large-scale functional networks in the mouse brain. Brain Structure and Function, 2016, 221, 3067-3079.	1.2	31
105	Does Anoxia Induce Cell Swelling in Carp Brains? In Vivo MRI Measurements in Crucian Carp and Common Carp. Journal of Neurophysiology, 2001, 85, 125-133.	0.9	30
106	Non-invasive PET imaging of brain inflammation at disease onset predicts spontaneous recurrent seizures and reflects comorbidities. Brain, Behavior, and Immunity, 2017, 61, 69-79.	2.0	30
107	Perineuronal nets and vocal plasticity in songbirds: A proposed mechanism to explain the difference between closedâ€ended and openâ€ended learning. Developmental Neurobiology, 2017, 77, 975-994.	1.5	30
			_

108Neural Correlates of Behavioural Olfactory Sensitivity Changes Seasonally in European Starlings.1.129108PLoS ONE, 2010, 5, e14337.1.129

#	Article	IF	CITATIONS
109	A complementary diffusion tensor imaging (DTI)-histological study in a model of Huntington's disease. Neurobiology of Aging, 2012, 33, 945-959.	1.5	29
110	Functional changes between seasons in the male songbird auditory forebrain. Frontiers in Behavioral Neuroscience, 2013, 7, 196.	1.0	29
111	The strengths of in vivo magnetic resonance imaging (MRI) to study environmental adaptational physiology in fish. Magnetic Resonance Materials in Physics, Biology, and Medicine, 2004, 17, 236-248.	1.1	28
112	Preserved Modular Network Organization in the Sedated Rat Brain. PLoS ONE, 2014, 9, e106156.	1.1	28
113	A patchy horizontal organization of the somatosensory activation of the rat cerebellum demonstrated by functional MRI. European Journal of Neuroscience, 1999, 11, 2720-2730.	1.2	27
114	Diffusion-weighted MRI of infarct growth in a rat photochemical stroke model: effect of lubeluzole. Neuropharmacology, 2000, 39, 691-702.	2.0	27
115	Topography and Lateralized Effect of Acute Aromatase Inhibition on Auditory Processing in a Seasonal Songbird. Journal of Neuroscience, 2017, 37, 4243-4254.	1.7	27
116	Functional MRI of Auditory Responses in the Zebra Finch Forebrain Reveals a Hierarchical Organisation Based on Signal Strength but Not Selectivity. PLoS ONE, 2008, 3, e3184.	1.1	26
117	A customizable 3-dimensional digital atlas of the canary brain in multiple modalities. NeuroImage, 2011, 57, 352-361.	2.1	26
118	Noninvasive Relative Quantification of [11C]ABP688 PET Imaging in Mice Versus an Input Function Measured Over an Arteriovenous Shunt. Frontiers in Neurology, 2018, 9, 516.	1.1	26
119	Molecular Imaging of Immune Cell Dynamics During De- and Remyelination in the Cuprizone Model of Multiple Sclerosis by [¹⁸ F]DPA-714 PET and MRI. Theranostics, 2019, 9, 1523-1537.	4.6	26
120	Special designed RF-antenna with integrated non-invasive carbon electrodes for simultaneous magnetic resonance imaging and electroencephalography acquisition at 7T. Magnetic Resonance Imaging, 2000, 18, 887-891.	1.0	25
121	The influence of light on the hatching of Artemia cysts (Anostraca:Branchiopoda:Crustacea). Journal of Experimental Marine Biology and Ecology, 1985, 92, 207-214.	0.7	24
122	Brain studies of mouse models for neurogenetic disorders using in vivo magnetic resonance imaging (MRI). European Journal of Human Genetics, 2001, 9, 153-159.	1.4	24
123	Measuring brain hemodynamic changes in a songbird: responses to hypercapnia measured with functional MRI and near-infrared spectroscopy. Physics in Medicine and Biology, 2008, 53, 2457-2470.	1.6	24
124	Resting-state functional MRI and [18F]-FDG PET demonstrate differences in neuronal activity between commonly used mouse strains. NeuroImage, 2016, 125, 571-577.	2.1	24
125	Timing of perineuronal net development in the zebra finch song control system correlates with developmental song learning. Proceedings of the Royal Society B: Biological Sciences, 2018, 285, 20180849.	1.2	24
126	Effects of sublethal copper exposure on muscle energy metabolism of common carp, measured by ³¹ Pâ€nuclear magnetic resonance spectroscopy. Environmental Toxicology and Chemistry, 1997, 16, 676-684.	2.2	23

#	Article	IF	CITATIONS
127	Recognition of cellular implants by the brain's innate immune system. Immunology and Cell Biology, 2011, 89, 511-516.	1.0	23
128	Multimodal in vivoimaging reveals limited allograft survival, intrapulmonary cell trapping and minimal evidence for ischemia-directed BMSC homing. BMC Biotechnology, 2012, 12, 93.	1.7	23
129	Tackling the physiological barriers for successful mesenchymal stem cell transplantation into the central nervous system. Stem Cell Research and Therapy, 2013, 4, 101.	2.4	23
130	Network structure of functional hippocampal lateralization in birds. Hippocampus, 2015, 25, 1418-1428.	0.9	23
131	Genotype specific age related changes in a transgenic rat model of Huntington's disease. NeuroImage, 2011, 58, 1006-1016.	2.1	22
132	Own Song Selectivity in the Songbird Auditory Pathway: Suppression by Norepinephrine. PLoS ONE, 2011, 6, e20131.	1.1	22
133	Magnetization transfer contrast imaging reveals amyloid pathology in Alzheimer's disease transgenic mice. Neurolmage, 2014, 87, 111-119.	2.1	22
134	A three-dimensional digital atlas of the starling brain. Brain Structure and Function, 2016, 221, 1899-1909.	1.2	22
135	Implementation of spinâ€echo blood oxygen levelâ€dependent (BOLD) functional MRI in birds. NMR in Biomedicine, 2010, 23, 1027-1032.	1.6	21
136	Labeling of Luciferase/eGFP-Expressing Bone Marrow-Derived Stromal Cells with Fluorescent Micron-Sized Iron Oxide Particles Improves Quantitative and Qualitative Multimodal Imaging of Cellular Grafts In Vivo. Molecular Imaging and Biology, 2011, 13, 1133-1145.	1.3	21
137	<i>In situ</i> labeling and imaging of endogenous neural stem cell proliferation and migration. Wiley Interdisciplinary Reviews: Nanomedicine and Nanobiotechnology, 2012, 4, 663-679.	3.3	20
138	Cuprizoneâ€induced demyelination and demyelinationâ€associated inflammation result in different proton magnetic resonance metabolite spectra. NMR in Biomedicine, 2015, 28, 505-513.	1.6	20
139	Clinical and immunological control of experimental autoimmune encephalomyelitis by tolerogenic dendritic cells loaded with MOG-encoding mRNA. Journal of Neuroinflammation, 2019, 16, 167.	3.1	20
140	Action spectroscopy of light-induced hatching ofArtemia cysts (Branchiopoda: Crustacea). Marine Biology, 1986, 91, 239-243.	0.7	19
141	Automatic localization of EEG electrode markers within 3D MR data. Magnetic Resonance Imaging, 2000, 18, 485-488.	1.0	19
142	Neuroadaptive responses to citalopram in rats using pharmacological magnetic resonance imaging. Psychopharmacology, 2011, 213, 521-531.	1.5	19
143	Current state-of-the-art of auditory functional MRI (fMRI) on zebra finches: Technique and scientific achievements. Journal of Physiology (Paris), 2013, 107, 156-169.	2.1	19
144	Early Inflammatory Responses following Cell Grafting in the CNS Trigger Activation of the Subventricular Zone: A Proposed Model of Sequential Cellular Events. Cell Transplantation, 2015, 24, 1481-1492.	1.2	19

#	Article	IF	CITATIONS
145	In vivo measurement of brain network connectivity reflects progression and intrinsic disease severity in a model of temporal lobe epilepsy. Neurobiology of Disease, 2019, 127, 45-52.	2.1	19
146	Increased soluble amyloid-beta causes early aberrant brain network hypersynchronisation in a mature-onset mouse model of amyloidosis. Acta Neuropathologica Communications, 2019, 7, 180.	2.4	19
147	A comparison between blood oxygenation level-dependent and cerebral blood volume contrast in the rat cerebral and cerebellar somatosensoric cortex during electrical paw stimulation. Journal of Magnetic Resonance Imaging, 2005, 22, 483-491.	1.9	18
148	Subchronic memantine induced concurrent functional disconnectivity and altered ultra-structural tissue integrity in the rodent brain: revealed by multimodal MRI. Psychopharmacology, 2013, 227, 479-491.	1.5	18
149	Metabolic Profiling of Dividing Cells in Live Rodent Brain by Proton Magnetic Resonance Spectroscopy (1HMRS) and LCModel Analysis. PLoS ONE, 2014, 9, e94755.	1.1	18
150	Exploring sex differences in the adult zebra finch brain: In vivo diffusion tensor imaging and ex vivo super-resolution track density imaging. NeuroImage, 2017, 146, 789-803.	2.1	18
151	Song Processing in the Zebra Finch Auditory Forebrain Reflects Asymmetric Sensitivity to Temporal and Spectral Structure. Frontiers in Neuroscience, 2017, 11, 549.	1.4	18
152	Development of a ligand for in vivo imaging of mutant huntingtin in Huntington's disease. Science Translational Medicine, 2022, 14, eabm3682.	5.8	18
153	Light-induced release ofArtemia dried embryos from diapause: Analysis of metabolic status. The Journal of Experimental Zoology, 1988, 247, 131-138.	1.4	17
154	A data post-processing protocol for dynamic MRI data to discriminate brain activity from global physiological effects. Magnetic Resonance Imaging, 2002, 20, 503-510.	1.0	17
155	Representation of Early Sensory Experience in the Adult Auditory Midbrain: Implications for Vocal Learning. PLoS ONE, 2013, 8, e61764.	1.1	17
156	A Panel of Trypanosoma brucei Strains Tagged with Blue and Red-Shifted Luciferases for Bioluminescent Imaging in Murine Infection Models. PLoS Neglected Tropical Diseases, 2014, 8, e3054.	1.3	17
157	Monitoring Blood-Brain Barrier Integrity Following Amyloid-β Immunotherapy Using Gadolinium-Enhanced MRI in a PDAPP Mouse Model. Journal of Alzheimer's Disease, 2016, 54, 723-735.	1.2	17
158	In Vivo Interleukin-13-Primed Macrophages Contribute to Reduced Alloantigen-Specific T Cell Activation and Prolong Immunological Survival of Allogeneic Mesenchymal Stem Cell Implants. Stem Cells, 2016, 34, 1971-1984.	1.4	17
159	MR-based spatial normalization improves [18F]MNI-659 PET regional quantification and detectability of disease effect in the Q175 mouse model of Huntington's disease. PLoS ONE, 2018, 13, e0206613.	1.1	17
160	Can longâ€distance migratory birds adjust to the advancement of spring by shortening migration distance? The response of the pied flycatcher to latitudinal photoperiodic variation. Global Change Biology, 2008, 14, 2516-2522.	4.2	16
161	Stem cell therapy for multiple sclerosis: preclinical evidence beyond all doubt?. Regenerative Medicine, 2012, 7, 245-259.	0.8	16
162	Acquisition of Spatial Search Strategies and Reversal Learning in the Morris Water Maze Depend on Disparate Brain Functional Connectivity in Mice. Cerebral Cortex, 2019, 29, 4519-4529.	1.6	16

#	Article	IF	CITATIONS
163	<i>In Vivo</i> Longitudinal Monitoring of Changes in the Corpus Callosum Integrity During Disease Progression in a Mouse Model of Alzheimer's Disease. Current Alzheimer Research, 2015, 12, 941-950.	0.7	16
164	Complementary use of T2-weighted and postcontrast T1- and T2â^—-weighted imaging to distinguish sites of reversible and irreversible brain damage in focal ischemic lesions in the rat brain. Magnetic Resonance Imaging, 1995, 13, 185-192.	1.0	15
165	Osmoregulation of the common carp (Cyprinus carpio) when exposed to an osmotic challenge assessed in-vivo and non-invasively by diffusion- and T2-weighted magnetic resonance imaging. Comparative Biochemistry and Physiology Part A, Molecular & Integrative Physiology, 1999, 124, 343-352.	0.8	15
166	IR-SE and IR-MEMRI allowin vivo visualization of oscine neuroarchitecture including the main forebrain regions of the song control system. NMR in Biomedicine, 2006, 19, 18-29.	1.6	15
167	Accelerated redevelopment of vocal skills is preceded by lasting reorganization of the song motor circuitry. ELife, 2019, 8, .	2.8	15
168	Recovery of the energy metabolism after a hypoxic challenge at different temperature conditions: a 31P-nuclear magnetic resonance spectroscopy study with common carp. Comparative Biochemistry and Physiology Part A, Molecular & Integrative Physiology, 1998, 120, 143-150.	0.8	14
169	Love songs, bird brains and diffusion tensor imaging. NMR in Biomedicine, 2010, 23, 873-883.	1.6	14
170	Background migration of USPIO/MLs is a major drawback for <i>in situ</i> labeling of endogenous neural progenitor cells. Contrast Media and Molecular Imaging, 2011, 6, 1-6.	0.4	14
171	Assessment of bystander killing-mediated therapy of malignant brain tumors using a multimodal imaging approach. Stem Cell Research and Therapy, 2015, 6, 163.	2.4	14
172	Image-guided phenotyping of ovariectomized mice: altered functional connectivity, cognition, myelination, and dopaminergic functionality. Neurobiology of Aging, 2019, 74, 77-89.	1.5	14
173	In vivo online monitoring of testosterone-induced neuroplasticity in a female songbird. Hormones and Behavior, 2020, 118, 104639.	1.0	14
174	In vitro NMR micro imaging of the spinal cord of chronic relapsing EAE rats. Magnetic Resonance Imaging, 1994, 12, 469-475.	1.0	13
175	Qualitative study ofin vivo melphalan adduct formation in the rat by miniaturized column-switching liquid chromatography coupled with electrospray mass spectrometry. Journal of Mass Spectrometry, 2004, 39, 29-37.	0.7	13
176	Activation of a sensorimotor pathway in response to a water temperature drop in a teleost fish. Journal of Experimental Biology, 2006, 209, 2015-2024.	0.8	13
177	Resting Brain Fluctuations Are Intrinsically Coupled to Visual Response Dynamics. Cerebral Cortex, 2021, 31, 1511-1522.	1.6	13
178	Resting-State Co-activation Patterns as Promising Candidates for Prediction of Alzheimer's Disease in Aged Mice. Frontiers in Neural Circuits, 2020, 14, 612529.	1.4	13
179	Entrapment of a neutral Tm(III)â€based complex with two innerâ€sphere coordinated water molecules into PEGâ€stabilized vesicles: towards an alternative strategy to develop highâ€performance LipoCEST contrast agents for MR imaging. Contrast Media and Molecular Imaging, 2014, 9, 391-399.	0.4	12
180	Neuroplasticity in the cerebello-thalamo-basal ganglia pathway: AÂlongitudinal in vivo MRI study in male songbirds. NeuroImage, 2018, 181, 190-202.	2.1	12

#	Article	IF	CITATIONS
181	Longitudinal evaluation of demyelinated lesions in a multiple sclerosis model using ultrashort echo time magnetization transfer (UTE-MT) imaging. NeuroImage, 2020, 208, 116415.	2.1	12
182	Complementary use of T2- and postcontrast T1-weighted NMR images for the sequential monitoring of focal ischemic lesions in the rat brain. Magnetic Resonance Imaging, 1993, 11, 675-683.	1.0	11
183	Water household of the common carp,Cyprinus carpio, when submitted to an osmotic challenge, as determined by diffusion-weighted magnetic resonance imaging at 7 T. Magnetic Resonance Materials in Physics, Biology, and Medicine, 1997, 5, 13-19.	1.1	11
184	Hypersynchronicity in the default mode-like network in a neurodevelopmental animal model with relevance for schizophrenia. Behavioural Brain Research, 2019, 364, 303-316.	1.2	11
185	First results of a quantitative study of DNA adducts of melphalan in the rat by isotope dilution mass spectrometry using capillary liquid chromatography coupled to electrospray tandem mass spectrometry. Rapid Communications in Mass Spectrometry, 2005, 19, 1999-2004.	0.7	10
186	Morphologic and functional changes in the unilateral 6-hydroxydopamine lesion rat model for Parkinson's disease discerned withÂμSPECT and quantitative MRI. Magnetic Resonance Materials in Physics, Biology, and Medicine, 2010, 23, 65-75.	1.1	10
187	An adaptive non local maximum likelihood estimation method for denoising magnetic resonance images. , 2012, , .		10
188	Effect of pH on the biological availability of copper to the brine shrimp Artemia franciscana. Marine Biology, 1988, 98, 31-38.	0.7	9
189	Phosphorylation, protein kinases and ADPKD. Biochimica Et Biophysica Acta - Molecular Basis of Disease, 2011, 1812, 1219-1224.	1.8	9
190	Multimodal imaging of micronâ€sized iron oxide particles following <i>in vitro</i> and <i>in vivo</i> uptake by stem cells: down to the nanometer scale. Contrast Media and Molecular Imaging, 2014, 9, 400-408.	0.4	9
191	A genome-wide search for epigenetically regulated genes in zebra finch using MethylCap-seq and RNA-seq. Scientific Reports, 2016, 6, 20957.	1.6	9
192	Bottom-up sensory processing can induce negative BOLD responses and reduce functional connectivity in nodes of the default mode-like network in rats. NeuroImage, 2019, 197, 167-176.	2.1	9
193	Progressive tau aggregation does not alter functional brain network connectivity in seeded hTau.P301L mice. Neurobiology of Disease, 2020, 143, 105011.	2.1	9
194	TSPO PET upregulation predicts epileptic phenotype at disease onset independently from chronic TSPO expression in a rat model of temporal lobe epilepsy. NeuroImage: Clinical, 2021, 31, 102701.	1.4	9
195	Functional magnetic resonance imaging in rodents: an unique tool to study in vivo pharmacologic neuromodulation. Current Opinion in Pharmacology, 2013, 13, 813-820.	1.7	8
196	Injury-Dependent Retention of Intraportally Administered Mesenchymal Stromal Cells Following Partial Hepatectomy of Steatotic Liver Does Not Lead to Improved Liver Recovery. PLoS ONE, 2013, 8, e69092.	1.1	8
197	Preclinical Comparison of the Amyloid-β Radioligands [11C]Pittsburgh compound B and [18F]florbetaben in Aged APPPS1-21 and BRI1-42 Mouse Models of Cerebral Amyloidosis. Molecular Imaging and Biology, 2015, 17, 688-696.	1.3	8
198	A three-dimensional digital neurological atlas of the mustached bat (Pteronotus parnellii). NeuroImage, 2018, 183, 300-313.	2.1	8

#	Article	IF	CITATIONS
199	DNA Methylation Regulates Transcription Factor-Specific Neurodevelopmental but Not Sexually Dimorphic Gene Expression Dynamics in Zebra Finch Telencephalon. Frontiers in Cell and Developmental Biology, 2021, 9, 583555.	1.8	8
200	In vivo assessment of the neural substrate linked with vocal imitation accuracy. ELife, 2020, 9, .	2.8	8
201	Auditory evoked BOLD responses in awake compared to lightly anaesthetized zebra finches. Scientific Reports, 2017, 7, 13563.	1.6	7
202	In Vivo Preclinical Molecular Imaging of Repeated Exposure to an <i>N</i> -methyl-d-aspartate Antagonist and a Glutaminase Inhibitor as Potential Glutamatergic Modulators. Journal of Pharmacology and Experimental Therapeutics, 2019, 368, 382-390.	1.3	7
203	Long-term ovarian hormone deprivation alters functional connectivity, brain neurochemical profile and white matter integrity in the Tg2576 amyloid mouse model of Alzheimer's disease. Neurobiology of Aging, 2021, 102, 139-150.	1.5	7
204	Histological Characterization and Quantification of Cellular Events Following Neural and Fibroblast(-Like) Stem Cell Grafting in Healthy and Demyelinated CNS Tissue. Methods in Molecular Biology, 2014, 1213, 265-283.	0.4	7
205	Involvement of cyclic nucleotides in light-induced resumption of development ofArtemia embryos. The Journal of Experimental Zoology, 1991, 258, 312-321.	1.4	6
206	Diffusion tensor image up-sampling: a registration-based approach. Magnetic Resonance Imaging, 2010, 28, 1497-1506.	1.0	6
207	Neuroanatomical targets of reboxetine and bupropion as revealed by pharmacological magnetic resonance imaging. Psychopharmacology, 2011, 217, 549-557.	1.5	6
208	Multimodal Imaging of Stem Cell Implantation in the Central Nervous System of Mice. Journal of Visualized Experiments, 2012, , e3906.	0.2	6
209	Quantitative Evaluation of Stem Cell Grafting in the Central Nervous System of Mice by In Vivo Bioluminescence Imaging and Postmortem Multicolor Histological Analysis. Methods in Molecular Biology, 2013, 1052, 125-141.	0.4	6
210	Magnetization transfer contrast imaging detects early white matter changes in the APP/PS1 amyloidosis mouse model. NeuroImage: Clinical, 2016, 12, 85-92.	1.4	5
211	Rapid changes in auditory processing in songbirds following acute aromatase inhibition as assessed by fMRI. Hormones and Behavior, 2018, 104, 63-76.	1.0	5
212	Uncovering a †̃sensitive window' of multisensory and motor neuroplasticity in the cerebrum and cerebellum of male and female starlings. ELife, 2021, 10, .	2.8	5
213	Reduced brain volumes in mice expressing APP-Austrian mutation but not in mice expressing APP-Swedish–Austrian mutations. Neuroscience Letters, 2008, 447, 143-147.	1.0	4
214	Volumetric development of the zebra finch brain throughout the first 200 days of post-hatch life traced by in vivo MRI. NeuroImage, 2018, 183, 227-238.	2.1	4
215	Monitoring Neuronal Network Disturbances of Brain Diseases: A Preclinical MRI Approach in the Rodent Brain. Frontiers in Cellular Neuroscience, 2021, 15, 815552.	1.8	4
216	Noninvasive in vivo 13C-NMR spectroscopy of a 13C-labeled xenobiotic in the rat. Magnetic Resonance Imaging, 1992, 10, 975-981.	1.0	3

#	Article	IF	CITATIONS
217	Dynamic manganese-enhanced MRI signal intensity processing based on nonlinear mixed modeling to study changes in neuronal activity. Journal of Agricultural, Biological, and Environmental Statistics, 2005, 10, 170-183.	0.7	3
218	Functional Magnetic Resonance Imaging (fMRI) with Auditory Stimulation in Songbirds. Journal of Visualized Experiments, 2013, , .	0.2	3
219	Imaging birds in a bird cage: in-vivo FSE 3D MRI of bird brain. Magnetic Resonance Materials in Physics, Biology, and Medicine, 1998, 6, 22-27.	1.1	2
220	<title>Quantification of tumor microvascular permeability in human glioma xenografts using dynamic T1 MRI with Gadomer-17</title> . , 1999, , .		2
221	Robust estimation of the noise variance from background MR data. , 2006, , .		2
222	Susceptibility correction for improved tractography using high field DT-EPI. Proceedings of SPIE, 2008, , .	0.8	2
223	A new combined live wire and active surface approach for volume-of-interest segmentation. , 2009, , .		2
224	Different anesthesia regimes modulate the functional connectivity outcome in mice. Magnetic Resonance in Medicine, 2014, 72, spcone-spcone.	1.9	2
225	Salt stress and resistance to hypoxic challenges in the common carp (Cyprinus carpio L.). , 2000, 57, 761.		2
226	EFFECTS OF SUBLETHAL COPPER EXPOSURE ON MUSCLE ENERGY METABOLISM OF COMMON CARP, MEASURED BY 31P-NUCLEAR MAGNETIC RESONANCE SPECTROSCOPY. Environmental Toxicology and Chemistry, 1997, 16, 676.	2.2	2
227	High resolution NMR imaging: Gd-DTPA labeled enzyme as a probe for permeability studies in polyacrylamide gels. Magnetic Resonance Imaging, 1991, 9, 583-587.	1.0	1
228	<title>Volume quantization of the mouse cerebellum by semiautomatic 3D segmentation of magnetic resonance images</title> . , 1996, , .		1
229	High resolution magnetic resonance imaging application in anatomy: the extensor digitorum muscle insertion on the first phalanx. Magnetic Resonance Materials in Physics, Biology, and Medicine, 1997, 5, 21-27.	1.1	1
230	<title>MRI as a tool to study brain structure from mouse models for mental retardation</title> . , 1998, , .		1
231	<title>Adaptive anisotropic noise filtering for magnitude MR data</title> . , 1999, 3661, 1418.		1
232	Diffusion Tensor Images Upsampling: A Registration-Based Approach. , 2009, , .		1
233	Improved B0 field map estimation for high field EPI. Magnetic Resonance Imaging, 2010, 28, 441-450.	1.0	1
234	Longâ€ŧerm deprivation of ovarian hormones via ovariectomy alters functional connectivity, brain neurochemistry and white matter integrity in a mouse model of Alzheimer's disease. Alzheimer's and Dementia, 2020, 16, e037354.	0.4	1

#	Article	IF	CITATIONS
235	Validation of Dementia Models Employing Neuroimaging Techniques. Neuromethods, 2011, , 187-220.	0.2	1
236	Striatal Injury Induces Overall Brain Alteration at the Pallial, Thalamic, and Cerebellar Levels. Biology, 2022, 11, 425.	1.3	1
237	<title>Functional magnetic resonance imaging of the rat cerebellum during electrical stimulation of the fore- and hindpaw at 7 T</title> . , 1999, 3660, 408.		0
238	<title>Automatic detection of EEG electrode markers on 3D MR data</title> . , 2000, , .		0
239	<title>Quantitative characterization of the progression of focal brain ischemia in a rat photochemical stroke model using in-vivo MRI</title> . , 2000, 3978, 476.		Ο
240	<title>Automatic EEG signal restoration during simultaneous EEG/MR acquisitions</title> ., 2000, , .		0
241	<title>In-vivo study of the thermoregulation of the rat tail using magnetic resonance angiography
(MRA)</title> . , 2000, 3978, 466.		Ο
242	<title>Changes during pentetrazol-induced epilepsy in rat recorded by simultaneous EEG/MRI at
7T</title> . , 2000, 3978, 485.		0
243	Brain Imaging. , 0, , 233-256.		Ο
244	Non-rigid coregistration of diffusion kurtosis data. , 2010, , .		0
245	A novel plaque rupture model in mice. Vascular Pharmacology, 2012, 56, 313.	1.0	Ο
246	P4-366: MONITORING BLOOD-BRAIN-BARRIER DISRUPTION FOLLOWING ABETA IMMUNOTHERAPY USING GADOLINIUM-ENHANCED MRI IN A PDAPP MOUSE MODEL. , 2014, 10, P922-P923.		0
247	MRI. Handbook of Behavioral Neuroscience, 2018, 28, 457-479.	0.7	0
248	Normalized averaged range (nAR), a robust quantification method for MPIO-content. Journal of Magnetic Resonance, 2019, 300, 18-27.	1.2	0
249	Molecular correlates of hypothalamic development in songbird ontogeny in comparison with the telencephalon. FASEB Journal, 2020, 34, 4997-5015.	0.2	Ο
250	Investigation of the brain's functional connectivity in a rat model of spatial neglect-like deficits Frontiers in Neuroscience, 0, 12, .	1.4	0
251	In vivo assessment of glymphatic clearance by DCE-MRI as potential prognostic biomarker of Alzheimer's disease. Frontiers in Neuroscience, 0, 13, .	1.4	0
252	Increased Soluble Aβ in adult mice causes pathological brain network hypersynchronisation early after induction. Frontiers in Neuroscience, 0, 13, .	1.4	0